

## A Trip in Julia Space: Morphological Change of Complex Boundaries

Michael Hild and Masao Komura

*Kyoto College of Arts, Department of Computer Graphics*

**Keywords:** Julia set, fractal, morphology, non-linear process

'A Trip in Julia Space' is an animated color video film composed of a collection of computational fractal images which represent Julia sets. They were computed by using simple non-linear iterative processes. One section of the film demonstrates the continuous development of uncomplicated set boundaries in the complex plane into those highly complex fractal images which are known since Mandelbrot. The continuous change of the set boundaries' complexity is due to a continuous change of a process parameter. The images give the impression of being animated by continuously and simultaneously rotating the color assignment table for all pixels. The film sequences were photographed from a monitor screen in real-time.

### 1. Introduction

It was discovered by Mandelbrot that Julia sets of the non-linear process  $z \rightarrow z^2 + c$  lead to fractal boundaries in the complex plane (Mandelbrot 1980). This paper reports on the extension of the quadratic process  $z \rightarrow z^2 + c$  to  $z \rightarrow z^m + c$ , where  $m$  is a real-valued variable, and on a variation of it. The morphological change of the resulting maps is shown as  $m$  is varied over a range of values. Two images of another structurally different process are also presented. Finally, a simple technique for animating such images is briefly described.

### 2. Morphological change of maps of the non-linear process $z \rightarrow z^m + c$

First we consider the non-linear quadratic function

$$z_{n+1} = z_n^2 + c \quad (1)$$

---

2-116 Uryuyama Kitashirakawa Sakyo-ku, Kyoto 606

## Morphological Change of Complex Boundaries

where  $z_n = x_n + i y_n$                       complex variable  
 $c = p + i q = \text{const.}$                     complex constant  
 $n = \{0, 1, 2, \dots, \infty\}$

This function was first studied in detail by the mathematicians Julia and Fatou, and was recently brought back to our attention by Mandelbrot. If we choose the initial value  $z_0 = x_0 + i y_0$  and compute  $z_1$  by using the above transformation, then in turn use  $z_1$  as input and compute  $z_2$  and so on, we get a series of complex numbers  $z_0 \rightarrow z_1 \rightarrow z_2 \rightarrow z_3 \rightarrow z_4 \rightarrow \dots$ . The values of these numbers will depend on the initial value  $z_0$  and the complex constant  $c$ .

For a given  $c$ , there are initial values for which the average modulus increases gradually and eventually tends to infinity as the number of iterations tends to infinity. That is not always the case. For the same complex constant  $c$ , but some different initial value  $z_0$ , the computed points map onto previously computed points (or at least onto points which lie in the neighborhood of previous points). Interestingly,  $z_n$  will not tend to infinity, as the number of iterational steps tends to infinity. Fig. 1 provides an illustration of that. Please note that in Fig. 1, the points are connected by straight lines to show their relationship with each other.

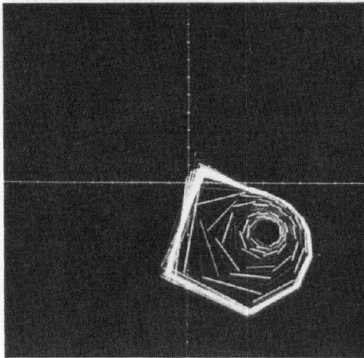


Fig. 1 : Attractor

Stable configurations of this kind are sometimes called 'strange attractors', while Mandelbrot recently prefers to call them 'fractal attractors' (Mandelbrot 1983). The presence of attractors suggests a search for all initial values  $z_0$ , for which they exist. It is also reasonable to record the number of iterational steps needed to reach a preset modulus  $B$  of  $z_n$  for all  $z_0$ . ( $B$  can be viewed as lying in the 'vicinity' of infinity). This method has been used by Peitgen & Richter (1985) and others. Whenever the value  $(x_n^2 + y_n^2)$  exceeds  $B$  for a given initial value  $z_0$ ,

$n$  (e.g., the number of iterational steps needed to reach  $B$ ) is assigned to its initial value  $z_0$ . Hence, the domain of initial values is mapped to the domain of iterational steps needed to reach the modulus  $B$ . This domain of iterational steps can be charted by using a color code to represent the number of iterational steps. By doing so, the plane will be covered by patches of different  $n$  (or colors); for the sake of simplicity, these patches are called  $n$ -patches in this paper. A typical map looks like the one in Fig. 15 (top right of Plate 3).

The color code that was used in the case of Fig. 15 is displayed at the bottom of the image. The colors to the left correspond to low numbers of iterational steps, while those to the right correspond to high numbers of iterational steps. In a region about the origin of the complex plane, the boundaries between  $n$ -patches are fractal. They can be thought of as being fractally deformed circles. The black patches include those initial values for which there exists an attractor, but not all

## Morphological Change of Complex Boundaries

of the black area points are 'attractor points'; this is due to the fact that  $n$  must be restricted to a finite value for practical purposes.

While the non-linear quadratic function has been studied extensively, very little is known about the function

$$z_{n+1} = z_n^m + c; \quad m = \{ R \mid 1.12, 1.14, \dots, 1.98 \}$$

$$\text{with } (x_n^2 + y_n^2) > B \quad \text{as condition} \quad (2)$$

e.g., using a real-valued exponent  $m$  instead of '2'. In general, this is the case of a multi-valued function, because of

$$z^m = r^m \exp(\varphi \cdot m + 2\pi k \cdot m) \quad (3)$$

where  $r$  : modulus of  $z$   
 $\varphi$  : phase angle of  $z$   
 $k = 0, \pm 1, \pm 2, \pm 3, \dots$

Usually, branch cuts are introduced to convert multi-valued functions into single-valued ones, but for the sake of comparing the cases of different (real)  $m$ -values that procedure is not so useful, since the number of needed branch cuts differs from  $m$  to  $m$ , and in some cases the number of branch cuts may become too high to be handled efficiently. The easiest procedure therefore is to further restrict the function to its principal value, e.g. to  $k = 0$ . Fig. 2 to Fig. 14 are maps obtained by this method. As described in the case of  $m = 2$ , the images have been computed using the same iteration method and the same constants  $c$  and  $B$ . For small  $m$ , the boundaries between  $n$ -patches are relatively simple and unspectacular. As  $m$  is increased, they become "rougher", while, like in the case of  $m = 2$ , self-similarity can be observed. The morphological change of the images with increasing  $m$  is continuous and quite naturally leads to the case  $m = 2$ . Global symmetry can not be observed, although their may be local ones in restricted regions. For  $m \leq 1.5$  there don't seem to exist attractors other than infinity, although for  $1.5 < m < 1.96$  attractors other than infinity do exist (black  $n$ -patches surrounded by lighter ones). Unlike the attractor one can observe for  $m = 2$  (whose points lie on a polygon with 11 vertices for  $c = 0.33 + i 0.043$ , see Fig. 1), the attractor (other than infinity) in the case of  $m \neq 2$  is a mere point and seems to be located in the 4th quadrant for all  $m$ 's. The attractor-regions appear to be connected, and their centers are located on logarithmic spirals. For  $1.96 \leq m < 2.0$  the process experiences severe changes since attractor-regions (for other-than-infinity-attractors) disappear momentarily and reappear for  $m = 2$  (see Fig. 13 and Fig. 14).

For the series of images presented in Fig. 16 to Fig. 23, basically the same non-linear process was used, but with an additional restriction. Whenever a mapped value ended up in the left half of the complex plane (negative real part of  $z_n$ ), its phase angle was advanced by  $\pi$  ( $\varphi_n + \pi$ ), e.g., the point symmetric to the origin in the right half of the complex plane

## Morphological Change of Complex Boundaries

was used as the next entry value to the process. For all the resulting images, point symmetry with respect to the origin can be observed. When beginning with low-valued  $m$ 's and gradually proceeding towards  $m = 2$ , the boundaries between  $n$ -patches first look very simple and similar to elements of Euclidian Geometry, but gradually become rougher, while displaying self-similarity, and finally evolve into the image of Fig. 15 ( $m = 2$ ). The morphological development of this series of maps is also continuous. Attractor-regions (other than infinity) were not found.

### 3. A different process

The following process leads to the images shown in Fig. 24 and Fig. 25.

$$\begin{aligned} z_{n+1} &= x_{n+1} + i \cdot y_{n+1}; \\ x_{n+1} &= r_n * \cos(\varphi_n * m) + p; \\ y_{n+1} &= r_n * \sin(\varphi_n * m) + q; \end{aligned} \quad (4)$$

$$\begin{aligned} \text{where } r_n &= (x_n^2 + y_n^2)^{\frac{m}{2}} \\ \varphi_n &= \tan(y_n / x_n) \end{aligned}$$

In the center of the complex plane a star-shaped region of  $n$ -patches, that appear randomly distributed, can be seen. But at the same time, those patches also appear to be subjected to an ordering force, similar to the well-known images of iron-powder scattered at random in a magnetic field. The  $n$ -patches more distant from the center are larger and display Euclidean-type boundaries. Quite interestingly, a modest change of scale does not seem to affect the nature of the distribution in the center, judging from close-up images by the scale factor 1:10. The question, whether the geometry of these images can be called 'fractal', must be left unanswered for the time being. When  $m$  is varied between  $m = 1.0$  (Fig. 24) and  $m = 2.7$  (Fig. 25), the resulting images also display a continuous morphological development. (The complete series of maps is not included in this paper).

### 4. On the experimental video film 'A Trip in Julia Space'

Most of the motifs used in the film were taken from the above described series of images. For a minority of others, different values of the complex constant  $c$  were used. Close-up images were also included. The first part of the film shows the morphological development of maps resulting from the described processes. The colors were mixed 'intuitively' and entered into a color assignment table. It was mentioned before, that the  $n$ -patches have been color-coded for the purpose of charting them; therefore any color combination can be used freely for making them visible. Since the  $n$ -patches of the images are made visible (and distinguishable) by assigning specific colors to each of the  $n$ -values, their appearance changes when the color assignment changes. Continuous changes in appearance can be achieved by 'rotating' the assignment table within certain limits. Therefore, all that is needed to convert this type of

## Morphological Change of Complex Boundaries

fractal static images into moving pictures is a high-speed graphics system. Every map was computed individually and then 'animated' by a color-change routine. All video-sequences were photographed from the monitor screen in real-time. For computations and high-speed display Apollo Domain DN660 graphic work stations were used.

### REFERENCES

- Mandelbrot, B.B. (1980): Fractal aspects of the iteration of  $z \rightarrow \lambda z(1-z)$  for complex  $\lambda$ ,  $z$ , Annals N.Y. Acad. Sciences, 357,249-259.  
Mandelbrot, B.B. (1983): The Fractal Geometry of Nature, Freeman, San Francisco, chapt. 20.  
Peitgen, H.-O., Richter, P.H. (1985): Schönheit im Chaos - Bilder aus der Theorie Komplexer Systeme, Forschungsgruppe Komplexe Dynamik, Universitaet Bremen.

### PLATES

(printed on Plate VII at the opening of this volume)

Series of maps resulting from process Eq. (2) and Eq. (3) with  $k=0$  :

On PLATE 1 :

Fig. 2 : $m = 1.10$ ;	Fig. 3 : $m = 1.20$ ;
Fig. 4 : $m = 1.30$ ;	Fig. 5 : $m = 1.40$ ;
Fig. 6 : $m = 1.50$ ;	Fig. 7 : $m = 1.60$ ;

On PLATE 2 :

Fig. 8 : $m = 1.70$ ;	Fig. 9 : $m = 1.80$ ;
Fig. 10 : $m = 1.90$ ;	Fig. 11 : $m = 1.92$ ;
Fig. 12 : $m = 1.94$ ;	Fig. 13 : $m = 1.96$ ;

On PLATE 3 :

Fig. 14 : $m = 1.98$ ;	Fig. 15 : $m = 2.00$ ;
------------------------	------------------------

Series of maps resulting from process Eq. (2) and Eq. (3) with  $k=0$  and the additional restriction  $\varphi_n := \varphi_n + \pi$  if  $\frac{\pi}{2} < \varphi_n < \frac{3\pi}{2}$  :

On PLATE 3 :

Fig. 16 : $m = 1.14$ ;	Fig. 17 : $m = 1.18$ ;
Fig. 18 : $m = 1.20$ ;	Fig. 19 : $m = 1.30$ ;

On PLATE 4 :

Fig. 20 : $m = 1.50$ ;	Fig. 21 : $m = 1.70$ ;
Fig. 22 : $m = 1.90$ ;	Fig. 23 : $m = 1.98$ ;
(Fig. 15 : $m = 2.00$ )	

Maps resulting from process Eq. (4) :

On PLATE 4 :

Fig. 24 : $m = 1.00$ ;	Fig. 25 : $m = 2.70$ ;
------------------------	------------------------

For all plate figures except Fig. 24, the same color code was used, but to a certain extent coloring inaccuracy was inevitable due to the photographic copying process. All figures display the range  $-2.0 < \text{Re}(z) < +2.0$  and  $-1.5 < \text{Im}(z) < +1.5$  of the Gaussian complex plane.

13-5

Q: I would like to know how you do your color assignment. Is there any rule for assigning color? And also about the background music: What is it? (N. Funakubo)

A: The meaning of 'color' in connection with the fractal maps used for the film is being discussed in my paper. Color assignment to "n-patches" is principally arbitrary; there is no rule. As for our movie, the color assignment was chosen to be visually attractive. The music is originally by [KECAK PELIATAN OF BALI], Indonesia, and was adopted to parts of the film by using effect such as echo etc.

Q: How did you make the rhythm of your motion picture? How did you take the time scale? Did it depend on your algorithm? (Y. Ito)

A: The visual rhythm of our motion picture depends on several factors: -on the morphological structure of the used map which in turn depends on the morphological process.

-on the color coding of "n-patches" (color assignment)

-on the speed and direction of the color assignment table's rotation.

The time scale was chosen arbitrarily and varies from film sequence to film sequence. In some instances, the scale also varies within a sequence.